Exponential Convergence Bounds in Least Squares Estimation: Identification of Viscoelastic Properties in Atomic Force Microscopy

Michael R. P. Ragazzon[1], J. Tommy Gravdahl[1], Kristin Y. Pettersen[2]

***Abstract*— Using atomic force microscopy (AFM) for studying soft, biological material has become increasingly popular in recent years. New approaches allow the use of recursive least squares estimation to identify the viscoelastic properties of a sample in AFM. As long as the regressor vector is persistently exciting (PE), exponential convergence of the parameters to be identified can be guaranteed. However, even exponential convergence can be slow. In this article, upper bounds on the parameter convergence is found, completely determined by the PE properties and least squares update law parameters. Furthermore, for a parameter vector which is piecewise constant at regular intervals, the time interval necessary for the error to converge to any specified upper limit is determined. For a soft sample in AFM, the viscoelastic properties can be spatially inhomogeneous. These properties can be spatially resolved by periodically tapping at discrete points along the sample. The results of this article then allows us to determine the time interval necessary at each tap in order to guarantee convergence to any specified fraction of the step-change in the parameters. Simulation results are presented, demonstrating the applicability of the approach.**

I. Introduction

Since its invention, atomic force microscopy (AFM) [1] has become one of the leading technologies for studying rigid materials at nano- to micrometer resolutions [2]. Over the last few decades it has increasingly been applied to studies of soft and biological matter at cellular and molecular scales [3], [4], [5]. The main advantages of AFM in this domain, can be attributed to its ability to image samples in their natural conditions, whether in air, buffers or other ambient media, such as allowing for direct imaging of living cells.

In AFM, a sharp tip attached to the end of a cantilever is lowered onto the sample. As the tip approaches the surface, the cantilever will start to deflect. This deflection can be measured in a photodector setup at high precision. The working principles of AFM essentially allow it to act as a force sensor in the pico-Newton ranges while mechanically interacting with samples [2]. This property of AFM has been utilized extensively to reveal static, mechanical properties of samples, in particular, elasticity [6], [7], [8].

Using AFM for identification of dynamic properties of samples, such as viscoelasticity, can be performed by modulating the loading force [9]. In such approaches, demodulated amplitude and phase of the deflection [10], [11], [12] are correlated to viscoelastic properties. More recently, multifrequency approaches have been employed for increased image acquisition rates [13], [14], [15], [16].

Another approach for imaging viscoelastic properties of soft matter using AFM was proposed in [17], based on modeling and parameter identification by a recursive least-squares algorithm (RLS) with forgetting factor [18]. The sample is then modeled as a spatially distributed grid of spring-damper elements to be identified. This approach can be operated in two distinct dynamic modes, both of which employ an oscillating cantilever. In dynamic indentation viscoelastic (DIVE) mode, the sample is periodically indented at discrete points across the sample [19]; while in scanning viscoelastic (SVE) mode, the cantilever is kept at a constant mean depth into the sample while scanning in a raster pattern [20].

In RLS, exponential convergence of the parameters can be guaranteed as long as the regressor signal is persistently exciting (PE) [18]. However, even exponential convergence can be slow. Thus, for practical implementations, knowledge of a guaranteed upper bound on the convergence rate is highly beneficial to the user. Furthermore, such an upper bound is a helpful tool in aiding the choice of update law parameters. In this article, an upper bound is presented which depends only on the PE properties and chosen update law parameters.

Another common practical consideration – often the reason for using recursive estimation approaches – is the time-varying nature of parameters and its effect on the parameter estimates. In general, exponential convergence in the constant parameter case, guarantees some degree of tracking for a sufficiently slowly-varying signal [21], [22]. The topic of time-varying parameters has been the focus of several studies [23], [24], [25], [26]. In DIVE mode identification using AFM [19], the viscoelastic properties of the sample are considered spatially inhomogeneous but constant in time. Accordingly, during each tap the parameters are constant, but for subsequent taps they can attain different constant values. Furthermore, the time interval between taps can be specified by the operator. Thus, a situation arises where the parameters are time-varying, piecewise constant, at a user-defined constant interval. In this article, by exploiting the exponential bounds that are derived for a constant parameter vector, the time interval necessary to converge to any specified upper limit of the error is determined. The results are applicable to any similar problem with a time-varying, piecewise constant parameter vector.

The article is organized as follows. First, the general

[1] M. R. P. Ragazzon and J. T. Gravdahl are with the Department of Engineering Cybernetics, NTNU, Norwegian University of Science and Technology, Trondheim, Norway. [2] K. Y. Pettersen is with the Centre for Autonomous Marine Operations and Systems (NTNU AMOS), Department of Engineering Cybernetics, NTNU. E-mail: {michael.remo.ragazzon, jan.tommy.gravdahl, kristin.y.pettersen}@ntnu.no.

framework for RLS is presented in Sec. II. The parameter convergence results with a constant and piecewise-constant parameter vector, respectively, is given in Sec. III. The theoretical results are applied to the viscoelastic identification problem in Sec. IV, before conclusions are given in Sec. V.

II. Recursive Least Squares Estimation

In this section, the general framework for RLS estimation is presented, applicable to a wide range of estimation problems. By adhering to the following setup of the plant model, RLS can easily be applied for estimation of the parameters. For further details, please see [18]. The described framework will be used as the foundation for the results of this article.

A. Plant Model

The plant model is described by the linearly parametrized system

$$z = \theta^{*T}\phi, \tag{1}$$

where $z \in \mathbb{R}$ is the input signal, $\theta^* \in \mathbb{R}^n$ is the vector of n unknown parameters, and $\phi \in \mathbb{R}^n$ is the known regressor vector. Furthermore, the estimation model is given by

$$\hat{z} = \theta^T\phi, \tag{2}$$

where $\hat{z} \in \mathbb{R}$ is the estimated input signal, and $\theta \in \mathbb{R}^n$ is the vector of estimated parameters. Furthermore, let the parameter estimation error be given by $\tilde{\theta} = \theta - \theta^*$.

B. Persistency of Excitation

The regressor vector ϕ is said to be persistently exciting (PE) if there exists constants, $\alpha_0, \alpha_1, T_0 > 0$ such that

$$\alpha_0 I \leq \frac{1}{T_0}\int_t^{t+T_0} \phi\phi^T d\tau \leq \alpha_1 I, \quad \forall t \geq 0. \tag{3}$$

where I is the identity matrix and α_0 is known as the level of excitation.

C. Least Squares Algorithm

Several methods exist for parameter estimation in models such as (1). The results of this article focus on the least-squares algorithm as described in the following. First consider the estimation error ε given by

$$\varepsilon = \frac{z - \hat{z}}{m^2} \tag{4}$$

$$m^2 = 1 + \alpha\phi^T\phi \tag{5}$$

where m^2 is a normalization signal which guarantees boundedness of the error, and $\alpha > 0$ is a design constant, typically unity.

The update law of the least-squares algorithm with forgetting factor is given by

$$\dot{\theta} = P\varepsilon\phi \tag{6}$$

$$\dot{P} = \beta P - \frac{P\phi\phi^T P}{m^2} \tag{7}$$

for some chosen value $\beta > 0$ and $P(0) = P_0 = P_0^T > 0$. In the remainder of the article, $|x|$ denotes the Euclidean norm of vector x.

III. Parameter Convergence

In this section, upper bounds on the parameter convergence are found for the parameter estimation problem specified in Sec. II. In particular, upper and lower bounds on $P(t)$ are derived which depend only on the PE properties and the chosen update law parameters. Then, these bounds are used to prove exponential convergence of a Lyapunov-like function and subsequently, to prove an exponential convergence rate of the parameter estimates in the case of constant parameters. Finally, the convergence rate in the piecewise-constant case follows.

A. Bounds on $P(t)$

Lemma 1. *If $m, \phi \in \mathscr{L}_\infty$, ϕ is PE, and θ^* is constant, then the least squares algorithm given by (4)-(7) guarantees the following bounds on $P(t)$:*

$$\gamma_1 I \leq P(t) \leq \gamma_2 I, \quad \forall t \geq 0 \tag{8}$$

with

$$\gamma_1 = \left(\lambda_{\min}(P_0)^{-1} + (\alpha\beta)^{-1}\right)^{-1} \tag{9}$$

$$\gamma_2 = \max\left\{\frac{\bar{m}^2}{\alpha_0 T_0}, \lambda_{\max}(P_0)\right\} e^{\beta T_0} \tag{10}$$

where $\bar{m}^2 = \sup_t m^2(t)$ and $\lambda_{\min}(\cdot), \lambda_{\max}(\cdot)$ denotes the minimum and maximum eigenvalue, respectively.

Proof. The proof closely follows the proof of [18, Cor. 4.3.2]. However, the bounds are here described in terms of $P(t)$ instead of Γ, and completely described by the constants of the framework in Sec. II. Specifically, (18) through (23) is new.

Denote $\Gamma = P^{-1}(t)$. Then, it can be shown that

$$\dot{\Gamma} = -\beta\Gamma + \frac{\phi\phi^T}{m^2}, \quad \Gamma(0) = \Gamma^T(0) = \Gamma_0 = P_0^{-1} \tag{11}$$

which gives

$$\Gamma(t) = e^{-\beta t}\Gamma_0 + \int_0^t e^{-\beta(t-\tau)}\frac{\phi(\tau)\phi(\tau)^T}{m^2(\tau)}d\tau. \tag{12}$$

Using the PE conditions (3) and $m \in \mathscr{L}_\infty$, we have for $t \geq T_0$,

$$\begin{aligned}\Gamma(t) &\geq \int_0^t e^{-\beta(t-\tau)}\frac{\phi(\tau)\phi(\tau)^T}{m^2(\tau)}d\tau \\ &= \int_{t-T_0}^t e^{-\beta(t-\tau)}\frac{\phi(\tau)\phi(\tau)^T}{m^2(\tau)}d\tau \\ &\quad + \int_0^{t-T_0} e^{-\beta(t-\tau)}\frac{\phi(\tau)\phi(\tau)^T}{m^2(\tau)}d\tau \qquad (13) \\ &\geq e^{-\beta T_0}\frac{\alpha_0 T_0}{\bar{m}^2} I. \qquad (14)\end{aligned}$$

For $t \leq T_0$, we have

$$\Gamma(t) \geq e^{-\beta T_0}\Gamma_0 \geq \lambda_{\min}(\Gamma_0)e^{-\beta T_0} I. \tag{15}$$

Then, combining (14)-(15), the lower bound is given by

$$\Gamma(t) \geq \eta_1 I, \quad \forall t \geq 0 \tag{16}$$

$$\eta_1 \triangleq \min\left\{\frac{\alpha_0 T_0}{\bar{m}^2}, \lambda_{\min}(\Gamma_0)\right\} e^{-\beta T_0}. \tag{17}$$

Next, an upper bound on $\Gamma(t)$ is sought. First, consider

$$\begin{aligned}\frac{\phi\phi^T}{m^2} &\leq \frac{\lambda_{\max}\left(\phi\phi^T\right)}{1+\alpha\phi^T\phi}I \\ &= \frac{\phi^T\phi}{1+\alpha\phi^T\phi}I \\ &\leq \frac{1}{\alpha}I. \end{aligned} \tag{18}$$

where $\lambda_{\max}\left(\phi\phi^T\right) = \phi^T\phi$ because $\phi\phi^T$ is a rank one matrix with an eigenvector given by ϕ, and the single eigenvalue follows. Combining (12) and (18) gives

$$\begin{aligned}\Gamma(t) &\leq \Gamma_0 + \int_0^t e^{-\beta(t-\tau)}\frac{1}{\alpha}Id\tau \\ &\leq \lambda_{\max}(\Gamma_0)I + \frac{1}{\alpha\beta}I \\ &= \eta_2 I \end{aligned} \tag{19}$$

where $\eta_2 \triangleq \lambda_{\max}(\Gamma_0) + \frac{1}{\alpha\beta}$.

Combining (16) and (19), gives

$$\eta_1 I \leq \Gamma(t) \leq \eta_2 I \tag{20}$$

$$\Updownarrow$$

$$\gamma_1 I \leq P(t) \leq \gamma_2 I \tag{21}$$

where

$$\gamma_1 = \eta_2^{-1} = \left(\lambda_{\min}(P_0)^{-1} + (\alpha\beta)^{-1}\right)^{-1} \tag{22}$$

$$\gamma_2 = \eta_1^{-1} = \max\left\{\frac{\bar{m}^2}{\alpha_0 T_0}, \lambda_{\max}(P_0)\right\} e^{\beta T_0} \tag{23}$$

which concludes the proof. □

B. Exponential Convergence

In this section, the bounds on $P(t)$ derived in Lemma 1 are used to prove exponential convergence of the Lyapunov-like function

$$V = \frac{\tilde{\theta}^T\Gamma\tilde{\theta}}{2}. \tag{24}$$

Please recall that $\tilde{\theta} \triangleq \theta - \theta^*$ and $\Gamma = P^{-1}(t)$.

Lemma 2. *If $m, \phi \in \mathscr{L}_\infty$, ϕ is PE, and θ^* is constant, then the least squares algorithm given by (6)-(7) guarantees that V from (24) decreases according to*

$$V(t+T_0) \leq \gamma V(t), \quad \forall t \geq 0 \tag{25}$$

with $0 < \gamma < 1$, where

$$\gamma = \frac{1-\mu}{1+\beta T_0} \tag{26}$$

$$\mu = \frac{\alpha_0 T_0 \gamma_1}{2\bar{m}^2 + \bar{\phi}^4 T_0^2 \gamma_2^2} \tag{27}$$

and $\bar{\phi} = \sup_t |\phi|$.

Proof. In [18, Sec. 4.8.3], the case of constant Γ was solved to find (25) with a different expression for γ. Here, the results are generalized to a time-varying Γ following a similar approach.

From the system description (1)-(5), the following relationships can be found

$$\varepsilon = \frac{z-\hat{z}}{m^2} = \frac{\theta^{*T}\phi - \theta^T\phi}{m^2} = -\frac{\tilde{\theta}^T\phi}{m^2} \tag{28}$$

such that

$$\varepsilon^2 m^2 = \frac{1}{m^2}\left(\tilde{\theta}^T\phi\right)^2. \tag{29}$$

Using V from (24) it can be shown that for a time-varying Γ [18, p. 199],

$$\dot{V} = -\frac{\varepsilon^2 m^2}{2} - \frac{\beta}{2}\tilde{\theta}^T\Gamma\tilde{\theta}. \tag{30}$$

Now, inserting for (24) and (29) into (30) gives

$$\dot{V} = -\frac{1}{2m^2}\left(\tilde{\theta}^T\phi\right)^2 - \beta V. \tag{31}$$

Now, we have

$$V(t+T) = V(t) - \int_t^{t+T}\left[\frac{(\tilde{\theta}(\tau)^T\phi(\tau))^2}{2m^2(\tau)} + \beta V(\tau)\right]d\tau. \tag{32}$$

Following the same procedure as for the constant Γ case [18, Sec. 4.8.3], but replacing the constant Γ by the bounds of Lemma 1 as appropriate, we have that the first term of the integral with $T = T_0$ is bounded by

$$\begin{aligned}\int_t^{t+T_0}\frac{(\tilde{\theta}(\tau)^T\phi(\tau))^2}{2m^2(\tau)}d\tau &\geq \frac{\alpha_0 T_0 \gamma_1}{2\bar{m}^2 + \bar{\phi}^4 T_0^2 \gamma_2^2}V(t) \\ &\triangleq \mu V(t). \end{aligned} \tag{33}$$

Since $V(t)$ is a non-increasing function, as seen from (30) with Γ positive definite, the second term of the integral (32) is bounded by

$$\int_t^{t+T}\beta V(\tau)d\tau \geq \beta T V(t+T). \tag{34}$$

Inserting (33) and (34) with $T = T_0$ into (32), we find

$$V(t+T_0) \leq V(t) - \mu V(t) - \beta T_0 V(t+T_0) \tag{35}$$

$$V(t+T_0) \leq \frac{1-\mu}{1+\beta T_0}V(t) \tag{36}$$

$$= \gamma V(t) \tag{37}$$

which concludes the proof. Since $\mu, \beta, T_0 > 0$ and $V(t) \geq 0$, it follows that $0 < \gamma < 1$. □

Since $\Gamma > 0$ and V decreases exponentially by Lemma 1–2, it follows that the parameter estimation error $\tilde{\theta}$ also decreases exponentially, as will be properly established in the following result.

Theorem 1. *Let $m, \phi \in \mathscr{L}_\infty$, ϕ be PE, and θ^* constant. Then, the least squares algorithm guarantees*

$$\left|\tilde{\theta}(t)\right| \leq a e^{-\lambda(t-t_0)}\left|\tilde{\theta}(t_0)\right|, \quad \forall t \geq t_0 \tag{38}$$

for any $t_0 \geq 0$, where the constants $a > 1, \lambda > 0$ are given by

$$a = \sqrt{\frac{\gamma_2}{\gamma\gamma_1}}, \quad \lambda = -\frac{\log\gamma}{2T_0}. \tag{39}$$

Furthermore, if $t_0 = 0$, a less conservative bound is given by

$$a = \sqrt{\frac{\gamma_2}{\gamma \lambda_{\min}(P_0)}}. \tag{40}$$

Proof. By recursively applying (25) it is clear that

$$V(t+t_0) \le V(nT_0+t_0) \le \gamma^n V(t_0), \quad \forall t \ge nT_0, \;\; n = 0,1,\dots \tag{41}$$

for any $t_0 \ge 0$. Now, it can be shown that the discrete γ^n can be upper bounded by the continuous expression,

$$\gamma^n \le \gamma^{-1} e^{t/T_0 \cdot \log \gamma}, \tag{42}$$

where the discrete and continuous expression intersect at the points $t = (n+1)T_0, \forall n \in \mathbb{N}$. Thus,

$$V(t+t_0) \le \gamma^{-1} e^{t/T_0 \cdot \log \gamma} V(t_0). \tag{43}$$

Furthermore, using Lemma 1, consider

$$V = \frac{\tilde{\theta}^T \Gamma \tilde{\theta}}{2} \ge \tfrac{1}{2}\eta_1 \tilde{\theta}^T \tilde{\theta} = \tfrac{1}{2}\eta_1 \left|\tilde{\theta}\right|^2. \tag{44}$$

Then, isolating $|\tilde{\theta}|$ and using (43) gives

$$\begin{aligned}
\left|\tilde{\theta}(t'+t_0)\right| &\le \sqrt{2\eta_1^{-1} V(t'+t_0)} && (45)\\
&\le \sqrt{2\gamma_2 \gamma^{-1} e^{t'/T_0 \cdot \log \gamma} V(t_0)} && (46)\\
&\le \sqrt{2\gamma_2 \gamma^{-1} e^{t'/T_0 \cdot \log \gamma} \tfrac{1}{2} \tilde{\theta}(t_0)^T \eta_2 \tilde{\theta}(t_0)} && (47)\\
&= \sqrt{\gamma_2 \gamma^{-1} \gamma_1^{-1}} e^{t'/(2T_0) \cdot \log \gamma} \left|\tilde{\theta}(t_0)\right| && (48)\\
&= a e^{-\lambda t'} \left|\tilde{\theta}(t_0)\right|, && (49)
\end{aligned}$$

where a, λ is given by (39). A change of coordinates by $t = t' + t_0$ gives (38). If $t_0 = 0$, then η_2 in (47) can be replaced by $\lambda_{\max}(\Gamma_0)$ and the less conservative a of (40) follows. Since $0 < \gamma < 1$, we have $\log \gamma < 0$ and in turn $\lambda > 0$. Furthermore, since $\gamma_1 \le \gamma_2, \gamma < 1$ then $a > 1$. □

C. Time-Varying Parameters

The exponential convergence of a constant parameter vector at an arbitrary initial time was established in Theorem 1. In the viscoelastic identification in AFM [19], the parameter vector is instead piecewise constant at regular intervals T. Convergence properties of the parameter estimates in this case, as well as insights for determining the interval, is desired and established in the following.

The parameter vector can now be described by

$$\theta^*(t) = \theta_i^*, \quad \forall \{t, i\} : t \in [t_i, t_{i+1}), i \in \mathbb{N}, t_i = iT \tag{50}$$

for some time interval $T > 0$ between successive values of the parameter vectors θ_i^*. The change between successive values of θ_i^* is assumed to be bounded by some constant Δ_{θ^*},

$$\left|\theta_i^* - \theta_{i-1}^*\right| \le \Delta_{\theta^*}, \quad \forall i. \tag{51}$$

Furthermore, the estimation error for θ_i^* is defined by

$$\tilde{\theta}_i \triangleq \theta(t_i + T) - \theta_i^* \tag{52}$$

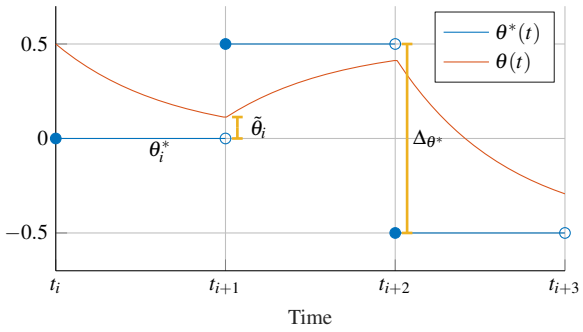

Fig. 1: Notation for piecewise constant parameters.

which is motivated by $\theta(t_i + T)$ being the last value estimated for $\theta^*(t) = \theta_i^*$. An example illustrating the notation used in this section is presented for a scalar case in Fig. 1.

Theorem 2. *Let $m, \phi \in \mathscr{L}_\infty$, ϕ be PE, and the parameter vector $\theta^*(t)$ be described by (50) and satisfy (51). Then, the least squares algorithm guarantees*

$$\left|\tilde{\theta}_i\right| \le \left(a e^{-\lambda T}\right)^{i+1} \left|\tilde{\theta}(0)\right| + \frac{\left(a e^{-\lambda T}\right)^i - 1}{a e^{-\lambda T} - 1} a e^{-\lambda T} \Delta_{\theta^*}, \; \forall i \in \mathbb{N}. \tag{53}$$

Furthermore, if $a e^{-\lambda T} < 1$, then, for large i,

$$\left|\tilde{\theta}_i\right| \le R \Delta_{\theta^*} \tag{54}$$

where $R = a e^{-\lambda T} / \left(1 - a e^{-\lambda T}\right)$. Conversely, for some specified $R > 0$, T is given by

$$T = \lambda^{-1} \log \frac{a(R+1)}{R}. \tag{55}$$

Proof. Using (38) in the intervals for which $\theta^*(t)$ is constant,

$$\left|\tilde{\theta}(t_i + T)\right| \le a e^{-\lambda T} \left|\tilde{\theta}(t_i)\right|, \quad \forall i \tag{56}$$

which can be applied recursively as in the following. For ease of notation let $\theta_i \triangleq \theta(t_i)$,

$$\begin{aligned}
\left|\tilde{\theta}_i\right| &= \left|\theta_{i+1} - \theta_i^*\right| \\
&\le a e^{-\lambda T} \left|\theta_i - \theta_i^*\right|, \\
&= a e^{-\lambda T} \left|\theta_i - \theta_{i-1}^* + \theta_{i-1}^* - \theta_i^*\right| \\
&\le a e^{-\lambda T} \left|\left|\theta_i - \theta_{i-1}^*\right| + \left|\Delta_{\theta^*}\right|\right| \\
&\le a e^{-\lambda T} \left|a e^{-\lambda T} \left|\theta_{i-1} - \theta_{i-1}^*\right| + \Delta_{\theta^*}\right| \\
&\le a e^{-\lambda T} \left|a e^{-\lambda T} \left(\left|\theta_{i-1} - \theta_{i-2}^*\right| + \Delta\theta^*\right) + \Delta\theta^*\right| \\
&= a e^{-\lambda T} \left|a e^{-\lambda T} \left|\theta_{i-1} - \theta_{i-2}^*\right| + \left(1 + a e^{-\lambda T}\right) \Delta_{\theta^*}\right| \\
&= a^2 e^{-2\lambda T} \left|\tilde{\theta}_{i-2}\right| + \left(a e^{-\lambda T} + a^2 e^{-2\lambda T}\right) \Delta_{\theta^*}
\end{aligned} \tag{57}$$

Recursively applying this n times until the initial condition $\left|\theta_0 - \theta_0^*\right| = \left|\tilde{\theta}(0)\right|$ appears and using the sum formula for the geometric series, gives

$$\left|\tilde{\theta}_i\right| \le a^{n+1} e^{-(n+1)\lambda T} \left|\tilde{\theta}(0)\right| + \frac{a^n e^{-\lambda n T} - 1}{a e^{-\lambda T} - 1} a e^{-\lambda T} \Delta_{\theta^*}, \tag{58}$$

which confirms (53). Furthermore, if $ae^{-\lambda T} < 1$, and by letting $n \to \infty$ such that the initial condition vanishes,

$$\left|\tilde{\theta}_n\right| \leq e^{-\infty}\left|\theta(t_0) - \theta_0^*\right| + \frac{ae^{-\lambda T}}{1-ae^{-\lambda T}}\Delta_{\theta^*} \tag{59}$$

$$= \frac{ae^{-\lambda T}}{1-ae^{-\lambda T}}\Delta_{\theta^*} \tag{60}$$

$$\triangleq R\Delta_{\theta^*} \tag{61}$$

where $R = ae^{-\lambda T}/(1-ae^{-\lambda T})$. Thus, if T can be controlled, the best estimate for each θ_i^* can be guaranteed to lie within any given fraction R of the maximum parameter step size, by solving R for T which trivially gives (55). Furthermore, it can be shown that T given by (55) automatically satisfies $ae^{-\lambda T} = R/(R+1) < 1$. □

Notably, for a sufficiently large interval T, the initial condition vanishes to zero after a sufficiently long time. Additionally, the estimation error reduces toward zero as T is increased.

IV. Case Study: Viscoelastic Identification in AFM

A. Problem Description

The primary motivation for developing the theory in the previous sections was for use in identification of viscoelastic sample properties in AFM operating in DIVE mode, as detailed in [17], [19]. The sample properties are modeled as laterally spaced spring-damper elements to be identified, as seen in Fig. 2. The sample is tapped into by the AFM tip at incrementing spatial coordinates, see Fig. 3, covering the entire sample grid by the end of the scan. Each tap is being performed at a constant lateral position for some chosen interval T. The problem reduces to estimating a time-varying, piecewise constant single pair of spring constant and damping coefficient.

In the following, the system dynamics are presented. The PE conditions for the system are developed, and following the theory developed in Section III, the choice of update law parameters of the least squares estimator are discussed. Furthermore, the interval T necessary to guarantee convergence of the parameters are presented as a function of the update law parameters.

B. System

The system can be described by [17], [19]

$$Ms^2Z - CsD - KD = (c^*s + k^*)\,\delta, \tag{62}$$

where M, C, K are the effective mass, damping coefficient and spring constant of the cantilever, respectively, and c^*, k^* are the unknown, piecewise constant parameters to be estimated. Furthermore,

$$Z = U - D, \quad \delta = h - Z \tag{63}$$

where Z is the vertical position of the cantilever tip, U is the vertical control input, D is the deflection of the cantilever, δ is the indentation of the tip into the sample,

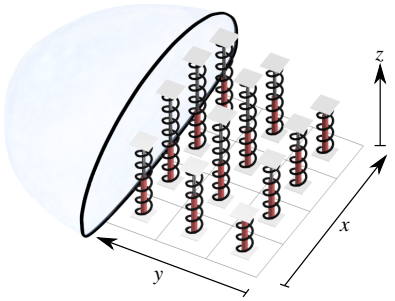

Fig. 2: The sample is modeled as spring-damper elements evenly spaced along the lateral axes.

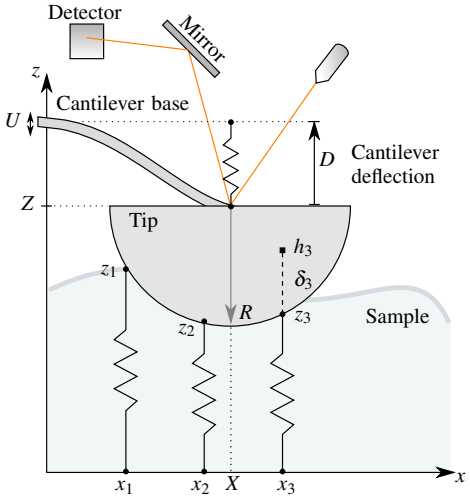

Fig. 3: Indentation of the cantilever tip into the sample.

and h is the topography height at the current lateral position of the cantilever tip (X, Y). The symbols are illustrated in Fig. 3. Additionally, there is a linear time-invariant (LTI) transformation from U to δ,

$$\delta(s) = -\frac{Cs + K}{Ms^2 + (C + c^*)s + (K + k^*)}U(s) \tag{64}$$

The parametric system (1) can now be set up as follows,

$$\theta^* = \begin{bmatrix} c^* & k^* \end{bmatrix}^T \tag{65}$$

$$\phi = \begin{bmatrix} s\delta & \delta \end{bmatrix}^T / \Lambda(s) \tag{66}$$

$$z = \left(Ms^2Z - CsD - KD\right)/\Lambda(s) \tag{67}$$

$$1/\Lambda(s) = 1/\left(\omega_c^{-1}s + 1\right)^2 \tag{68}$$

where $1/\Lambda(s)$ is a second-order low-pass filter with cut-off frequency ω_c introduced to make z, ϕ proper. Furthermore, U is a feedforward signal providing excitation to the system according to

$$U(t) = A'\sin(\omega t) + u_0, \tag{69}$$

for some constants u_0 and $A', \omega > 0$.

Using (64), (66), (68) it is seen that $\frac{\phi}{U}(s)$ is LTI and strictly proper. Thus, by using the excitation signal (69), there exist

some constants A, φ such that

$$\delta/\Lambda = A\sin(\omega t + \varphi) \tag{70}$$
$$s\delta/\Lambda = A\omega\cos(\omega t + \varphi) \tag{71}$$

where $A = \left|\frac{\phi_2}{U}(j\omega)\right| A'$ and $\varphi = \angle\frac{\phi_2}{U}(j\omega)$. Thus,

$$\phi = \begin{bmatrix} A\omega\cos(\omega t+\varphi) & A\sin(\omega t+\varphi) \end{bmatrix}^T \tag{72}$$

C. Persistency of Excitation

First, consider the PE expression from (3),

$$S \triangleq \frac{1}{T_0}\int_t^{t+T_0} \phi\phi^T d\tau. \tag{73}$$

By choosing

$$T_0 = \pi\omega^{-1} \tag{74}$$

and using (72), it can be shown that the solution to (73) is given by

$$S = \begin{bmatrix} \frac{1}{2}A^2\omega^2 & 0 \\ 0 & \frac{1}{2}A^2 \end{bmatrix}. \tag{75}$$

Thus, ϕ is PE with level of excitation α_0 and α_1 given by

$$\alpha_0 = \tfrac{1}{2}A^2\min\{\omega^2, 1\} \tag{76}$$
$$\alpha_1 = \tfrac{1}{2}A^2\max\{\omega^2, 1\} \tag{77}$$

which satisfies the PE condition

$$\alpha_0 I \le S \le \alpha_1 I. \tag{78}$$

D. Tuning and Convergence Rate

The RLS estimator (4)-(7) is implemented for the described system. Since ϕ is PE, exponential convergence of the parameters is guaranteed. By employing the theoretical results of Sec. III, the rate of convergence will be investigated in the following. We choose

$$\alpha = 1, \quad P_0 = p_0 I, \tag{79}$$

and will further investigate the choice of β and p_0 in the following. First, the following properties can be determined already, considering ϕ from (72)

$$\bar{\phi} = A\sqrt{\omega^2+1}, \;\; \bar{m}^2 = 1+\bar{\phi}^2, \;\; \lambda_{\min}(P_0) = \lambda_{\max}(P_0) = p_0. \tag{80}$$

Inserting these values and the constants from the PE conditions into (26),(27),(39), the upper bound on the exponential convergence λ and a can be found in terms of β, p_0, A, ω.

Remark 1. Note that A is implicitly a function of the system coefficients and transfer functions. However, since A is measurable through demodulation of the deflection signal D, and $A \propto A'$ with A' being operator-defined, it can be controlled to any desired value.

In the following, the upper limit of the convergence rate determined by a, λ will be investigated by the parameter estimator constants β, p_0. It will be used that $A = 50\,\text{nm}$, and $\omega = 2\pi f_0$ where $f_0 = 20\,\text{kHz}$, corresponding to the setup in [17].

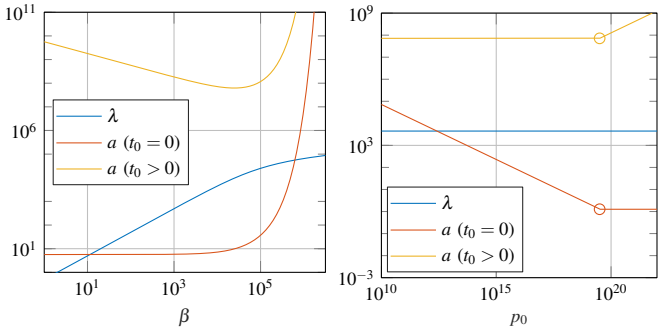

(a) β ($p_0 = 10^{18}$) (b) p_0 ($\beta = 10^4$)

Fig. 4: The exponential convergence rate λ, and multiplier a, as a function of β, p_0 of the least squares estimator.

In Fig. 4, the exponential convergence rate λ and multiplier a are plotted in terms of β, p_0. This gives valuable information into how the RLS estimator behaves. In the long run, the exponential rate λ will dominate the multiplier a and determine how fast the system converges. However, for a shorter run, a can in several cases become very large and thus lead to slow convergence. In both plots, a is plotted both for the conservative case (any initial time) and less conservative case (initial time zero), corresponding to (39),(40) respectively. In the former case, a does not go lower than approximately 10^8, a very high number which can be attributed to the necessity of considering the largest range in the bounds of $P(t)$. In the initial time zero case, the lower bound can be controlled by p_0, allowing for a decreasing range in the bounds of $P(t)$ and thus a smaller value of a with increasing p_0, as evident from Fig. 4(b). In fact, a becomes very close to unity for large values of p_0 and small values of β.

The plots in Fig. 4 can quickly be used to determine appropriate values of β, p_0. In general, λ increases with increasing β, but at some point, around $\beta = 10^4$, a starts to rapidly increase. On the other hand, λ does not change with p_0, but a reaches its minimum at $p_0 = \bar{m}^2/(\alpha_0 T_0) \approx 3\times 10^{19}$. Thus, $\beta = 10^4, p_0 = 3\times 10^{19}$ are appropriate choices for this problem.

In Fig. 5, the upper limit of the parameter error relative to the initial condition, or $ae^{-\lambda t}$ from (38), is plotted as a function of β. Due to the rapid increase in a for large values of β, but λ increasing for large β, there exists an optimal point for β providing the fastest convergence after a given time. E.g. at $t = 10T_0$, the error has reached about 1% of the initial error with $\beta = 3\times 10^5$.

For the piecewise constant parameter case, the time interval needed for reaching a given fraction R of the maximum parameter step size Δ_{θ^*} can be plotted as in Fig. 6. E.g., for $\beta = 10^2$, the time interval needed to reach 0.1% of Δ_{θ^*} is $T \approx 0.55\,\text{s}$.

E. Simulation

A simulation is performed in order to evaluate the correctness of the results of Sec. III. Additionally, since the

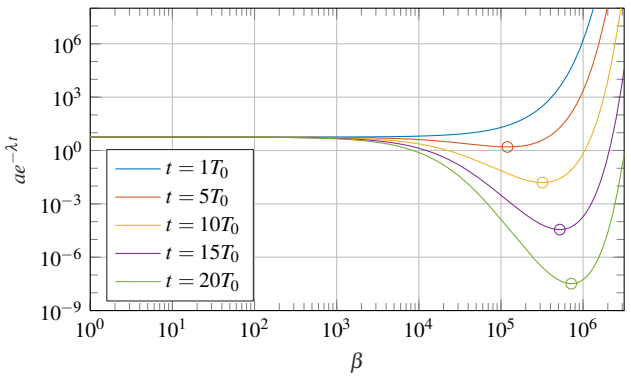

Fig. 5: Upper limit on convergence of parameter error after $t = nT_0$, as a function of β, with $t_0 = 0, p_0 = 10^{18}$. Circles mark minimum points.

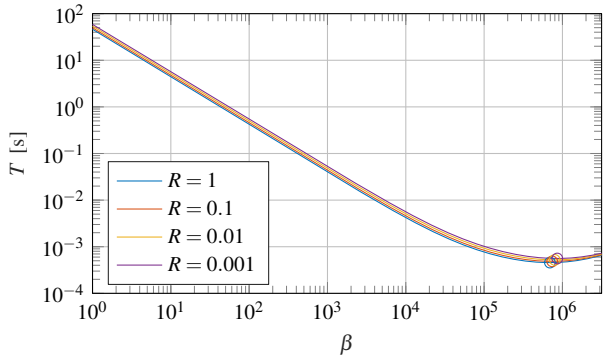

Fig. 6: Time-varying parameters: Minimum estimation interval T necessary to guarantee parameter estimate to within $R\Delta_{\theta^*}$ of real parameters, as a function of β.

presented convergence bounds are based on an inherently conservative approach, a simulation can establish how the actual performance compares to the upper bounds.

The simulation has been setup according to Fig. 7. The cantilever-sample dynamics are modeled by (62), with physical parameters from [17]. That is, $M = 1.18 \times 10^{-11}\,\mathrm{kg}$, $C = 1.5 \times 10^{-8}\,\mathrm{Ns/m}$, and $K = 0.19\,\mathrm{N/m}$, corresponding to a resonance frequency of 20 kHz. The cantilever oscillations were performed at a depth of 100 nm into the sample. The unknown spring constant and damping coefficient of the sample to be estimated, are piecewise constant corresponding to the lateral placement of the cantilever, with $\Delta_{\theta^*} = 0.01$. Only the vertical positioning U and deflection D are assumed available for measurement, corresponding to an actual AFM experiment.

A practical experiment would need to take into account noise when determining β. A very high value of β makes the estimator very sensitive to noise, since this leads to a larger value of $P(t)$ in general. To be representative of an experiment, a relatively low value was chosen with $\beta = 100$. On the other hand, we chose $p_0 = 10^{18}$. From Fig. 6, and by choosing $R = 0.001$, the time interval between taps needs to be at least 0.55 s, we chose $T = 0.6\,\mathrm{s}$ for the nearest

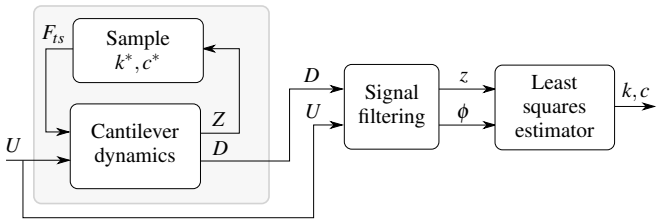

Fig. 7: Block diagram of the simulation setup, with cantilever-sample dynamics and parameter estimator.

round number. This should guarantee $|\tilde{\theta}_i| \leq 0.001\Delta_{\theta^*}$ by Theorem 2. The resulting convergence parameters for an arbitrary initial time is then given by

$$a = 5.6 \times 10^8, \quad \lambda = 49.9. \tag{81}$$

The results of the simulation are plotted in Fig. 8 and Fig. 9. The results are plotted from after an initial time $T_{\text{init}} = 0.6\,\mathrm{s}$ to let the initial conditions vanish. The parameter estimation of c and k compared to their real values are shown in Fig. 8, demonstrating the exponential convergence after each step-change in the parameters.

In Fig. 9 the parameter error norm is plotted, and compared to the upper limit between intervals as given by Theorem 1. It is seen that at the end of each interval, the upper bound reaches below $R\Delta_{\theta^*}$, in correspondence with Theorem 2. It is also seen that the real error stays below the upper bound, by a large offset. This can predominantly be attributed to the large value of a, which gives a very large offset at the beginning of each interval.

One approach to guarantee a lower bound at an arbitrary initial time, would be to perform a covariance reset at the beginning of each interval. That is, by setting $P(nT) = P_0$, which would essentially act as starting from $t_0 = 0$. This would lead to a value $a = 5.6$, or eight orders of magnitude smaller than for an arbitrary initial condition.

V. Conclusion

In this article, a recursive least squares (RLS) estimator with forgetting factor was investigated. An upper bound on the exponential convergence of the parameter estimation error – completely determined by the RLS parameters and the level of excitation of the regressor vector – is given by Theorem 1 for a constant parameter vector. Furthermore, the case of piecewise constant parameter vector at regular intervals was considered. An upper bound in this case – as given in Theorem 2 – relates the initial parameter error and maximum parameter step-size to the parameter error. Additionally, the necessary time interval for the parameters to converge to a given fraction of the maximum parameter step-change was presented. Finally, the theoretical results were applied to the problem of identification of viscoelastic properties using AFM. Choices of RLS parameters were discussed, and the minimum time interval necessary for guaranteed convergence to some specified value was found. Simulations corroborate the results and demonstrate the applicability of the approach.

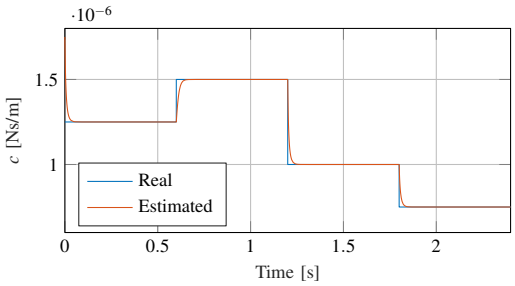

(a) c

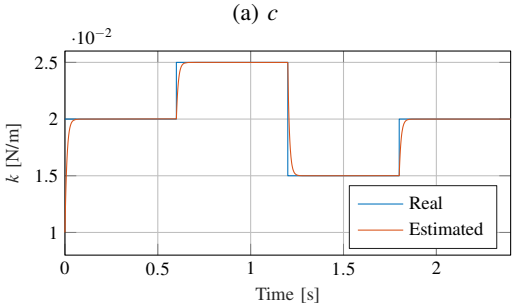

(b) k

Fig. 8: Simulated parameter estimation with parameters changing at regular intervals.

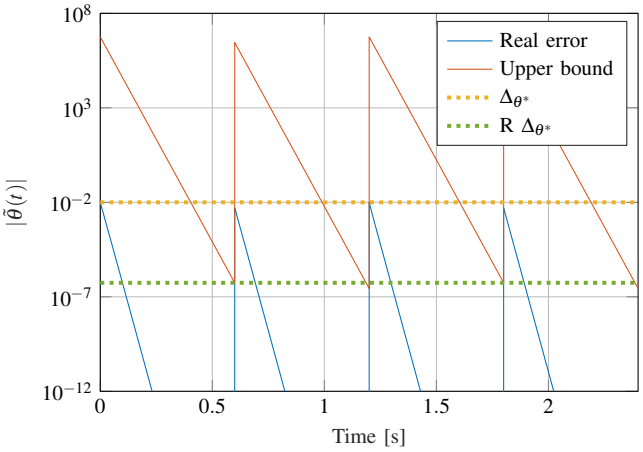

Fig. 9: Simulated parameter estimation error with parameters changing at regular intervals, compared to the pre-determined upper bound. After each interval, the upper bound guarantees convergence to less than $R\Delta_{\theta^*}$ with $R = 0.001$.

References

[1] G. Binnig, C. F. Quate, and C. Gerber, "Atomic Force Microscope," *Phys. Rev. Lett.*, vol. 56, no. 9, pp. 930–933, 1986.

[2] D. Y. Abramovitch, S. B. Andersson, L. Y. Pao, and G. Schitter, "A Tutorial on the Mechanisms, Dynamics, and Control of Atomic Force Microscopes," in *Proc. American Control Conference*, New York, USA, 2007, pp. 3488–3502.

[3] N. Jalili and K. Laxminarayana, "A review of atomic force microscopy imaging systems: application to molecular metrology and biological sciences," *Mechatronics*, vol. 14, no. 8, pp. 907–945, 2004.

[4] T. Uchihashi, H. Watanabe, S. Fukuda, M. Shibata, and T. Ando, "Functional extension of high-speed AFM for wider biological applications," *Ultramicroscopy*, vol. 160, pp. 182–196, 2016.

[5] T. Ando, T. Uchihashi, and N. Kodera, "High-speed AFM and applications to biomolecular systems." *Annual review of biophysics*, vol. 42, pp. 393–414, 2013.

[6] P. Carl and H. Schillers, "Elasticity measurement of living cells with an atomic force microscope: Data acquisition and processing," *Pflugers Archiv European Journal of Physiology*, vol. 457, no. 2, pp. 551–559, 2008.

[7] I. Sokolov, M. E. Dokukin, and N. V. Guz, "Method for quantitative measurements of the elastic modulus of biological cells in AFM indentation experiments," *Methods*, vol. 60, no. 2, pp. 202–213, 2013.

[8] N. Guz, M. Dokukin, V. Kalaparthi, and I. Sokolov, "If Cell Mechanics Can Be Described by Elastic Modulus: Study of Different Models and Probes Used in Indentation Experiments," *Biophysical Journal*, vol. 107, no. 3, pp. 564–575, 2014.

[9] M. Radmacher, R. W. Tillmann, and H. E. Gaub, "Imaging viscoelasticity by force modulation with the atomic force microscope." *Biophysical journal*, vol. 64, no. 3, pp. 735–742, 1993.

[10] M. R. P. Ragazzon, J. T. Gravdahl, and A. J. Fleming, "On Amplitude Estimation for High-Speed Atomic Force Microscopy," in *Proc. American Control Conference*, Boston, USA, 2016.

[11] M. G. Ruppert, D. M. Harcombe, M. R. P. Ragazzon, S. O. R. Moheimani, and A. J. Fleming, "A Review of Demodulation Techniques for Dynamic Mode Atomic Force Microscopy," *Beilstein journal of nanotechnology*, 2017, accepted for publication.

[12] M. R. P. Ragazzon, M. G. Ruppert, D. M. Harcombe, A. J. Fleming, and J. T. Gravdahl, "Lyapunov estimator for high-speed demodulation in dynamic mode atomic force microscopy," *IEEE Transactions on Control Systems Technology*, vol. PP, no. 99, pp. 1–8, 2017.

[13] A. Raman, S. Trigueros, A. Cartagena, A. P. Z. Stevenson, M. Susilo, E. Nauman, and S. A. Contera, "Mapping nanomechanical properties of live cells using multi-harmonic atomic force microscopy." *Nature nanotechnology*, vol. 6, no. 12, pp. 809–14, 2011.

[14] R. Garcia and R. Proksch, "Nanomechanical mapping of soft matter by bimodal force microscopy," *European Polymer Journal*, vol. 49, no. 8, pp. 1897–1906, 2013.

[15] A. Cartagena and A. Raman, "Local Viscoelastic Properties of Live Cells Investigated Using Dynamic and Quasi-Static Atomic Force Microscopy Methods," *Biophysical Journal*, vol. 106, no. 5, pp. 1033–1043, 2014.

[16] E. T. Herruzo, A. P. Perrino, and R. Garcia, "Fast nanomechanical spectroscopy of soft matter," *Nature communications*, vol. 5, p. 3126, 2014.

[17] M. R. P. Ragazzon, J. T. Gravdahl, and M. Vagia, "Viscoelastic Properties of Cells: Modeling and Identification by Atomic Force Microscopy," *Mechatronics*, 2017, provisionally accepted for publication.

[18] P. A. Ioannou and J. Sun, *Robust adaptive control*. Upper Saddle River, NJ: Prentice Hall, 1996.

[19] M. R. P. Ragazzon, M. Vagia, and J. T. Gravdahl, "Cell Mechanics Modeling and Identification by Atomic Force Microscopy," in *Proc. 7th IFAC Symposium on Mechatronic Systems*, Loughborough, UK, 2016.

[20] M. R. P. Ragazzon and J. T. Gravdahl, "Imaging Topography and Viscoelastic Properties by Constant Depth Atomic Force Microscopy," in *Proc. IEEE Multi-Conference on Systems and Control*, Buenos Aires, Argentina, 2016.

[21] B. D. O. Anderson and R. M. Johnstone, "Adaptive systems and time varying plants," *International Journal of Control*, vol. 37, no. 2, pp. 367–377, 1983.

[22] M. F. de Mathelin and R. Lozano, "Robust adaptive identification of slowly time-varying parameters with bounded disturbances," in *Proc. European Control Conference*, Brussels, Belgium, 1997, pp. 2300–2305.

[23] A. Vahidi, A. Stefanopoulou, and H. Peng, "Recursive least squares with forgetting for online estimation of vehicle mass and road grade: theory and experiments," *Vehicle System Dynamics*, vol. 43, no. 1, pp. 31–55, 2005.

[24] L. Ljung and S. Gunnarsson, "Adaptation and tracking in system identification-A survey," *Automatica*, vol. 26, no. 1, pp. 7–21, 1990.

[25] F. Ding and T. Chen, "Performance bounds of forgetting factor least-squares algorithms for time-varying systems with finite measurement data," *IEEE Transactions on Circuits and Systems I: Regular Papers*, vol. 52, no. 3, pp. 555–566, 2005.

[26] Y. Zhu and P. R. Pagilla, "Adaptive Estimation of Time-Varying Parameters in Linearly Parametrized Systems," *Journal of Dynamic Systems, Measurement, and Control*, vol. 128, no. 3, p. 691, 2006.